Eur. Phys. J. C 8, 473–478 (1999)
DOI 10.1007/s100529901105

THE EUROPEAN PHYSICAL JOURNAL C

Can one discriminate the thermal dilepton signal against the open charm and bottom decay background in ultrarelativistic heavy-ion collisions?

K. Gallmeister[1], B. Kämpfer[1], O.P. Pavlenko[1,2]

[1] Forschungszentrum Rossendorf, PF 510119, D-01314 Dresden, Germany
[2] Institute for Theoretical Physics, 252143 Kiev - 143, Ukraine

Received: 28 September 1998 / Revised version: 27 November 1998 / Published online: 22 March 1999

Abstract. In ultrarelativistic heavy-ion collisions at $\sqrt{s} > 20$ (120) A·GeV a copious production of charm (bottom) production sets in which, via correlated semileptonic $D\bar{D}$ ($B\bar{B}$) decays, gives rise to a dilepton yield at invariant mass $M \approx 2-3$ GeV in excess of the Drell-Yan yield and the thermal dilepton signal from deconfined matter as well. We show that appropriate single-electron transverse momentum cuts (suitable for ALICE at LHC) cause a threshold like behavior of the dilepton spectra from heavy-quark meson decays and the Drell-Yan process and can allow to observe a thermal dilepton signal from hot deconfined matter.

1 Introduction

The current relativistic heavy-ion experiments at CERN-SPS and planned future experiments at BNL-RHIC and CERN-LHC are aimed at a study of the properties of highly excited, deconfined matter. The production of dileptons with intermediate invariant mass in the so-called continuum region between ϕ and J/ψ are widely considered as one of the main tools to measure in such experiments the "initial" temperature and other thermodynamical characteristics of the produced matter [1,2]. Dilepton measurements are envisaged in particular with the PHENIX and ALICE detector facilities at RHIC and LHC, respectively. The thermal dilepton signal in the intermediate invariant mass region faces a serious background problem connected with hard initial quark - antiquark annihilation into dileptons (i.e. the Drell-Yan production). The general expectation is that with increasing beam energy the maximum temperature of matter rises and consequently the thermal dilepton yield grows faster than the Drell-Yan yield. However with increasing beam energy also a copious production of heavy quarks, resulting in hard initial collisions of partons too, sets in. As a consequence, the correlated semileptonic decays of open charm and bottom mesons yield a dilepton rate exceeding the one from the Drell-Yan process. This can be understood by the following simple arguments. Drell-Yan pairs are produced dominantly via $q\bar{q}$ annihilation, while the open charm and bottom production involves mainly gluons of colliding nuclei. Since the parton structure functions [3] point to a strong increase of the gluon density at small values of the below explained variable x, one can expect a corresponding increase of the relative contribution from charm and bottom decays into the intermediate mass region of dileptons with increasing beam energy or $\sqrt{s}$. Therefore it is *a priori* not obvious in which energy region one meets best conditions for observing a thermal dilepton signal from hot deconfined matter.

In this note we present a schematic view on the beam energy dependence of the mentioned sources of dileptons. Additionally we study systematically the influence of single-electron transverse momentum cuts on the invariant mass spectra of dileptons and show that at ALICE at LHC such cuts can suppress the Drell-Yan and correlated semileptonic decay dielectrons. Thus an observation of the thermal signal seems to be feasible, supposed the uncorrelated background can be accurately enough removed by like-sign subtraction.

2 Beam energy dependence of dilepton sources

Our basic equations for calculating the above mentioned dilepton sources can be found in [4,5] and are presented below in modified form. In Fig. 1 we show the beam energy dependence of the Drell-Yan yield and the yield from correlated $D\bar{D}$, $B\bar{B}$ decays in central Au + Au collisions. One infers from Fig. 1 that the ratio of Drell-Yan to open charm (bottom) decay dileptons with invariant mass $M =$ 2.5 GeV drops down with increasing $\sqrt{s}$. Only in the region $\sqrt{s} < 20$ (120) A·GeV the Drell-Yan yield dominates above the charm (bottom) decay contribution. Such a conclusion is in agreement with a recent analysis [6] which points out that the open charm source cannot explain the experimental data of CERES and NA38/NA50 of the dilepton spectra in S – U and Pb – Pb collisions at SPS energies.

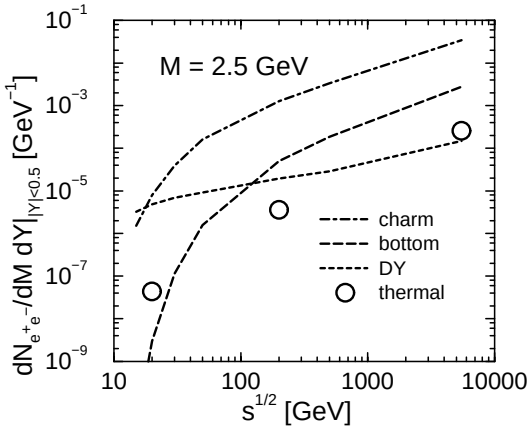

Fig. 1. The dependence of dileptons from the lowest-order Drell-Yan process, and correlated open charm and bottom decays and the thermal source (only purely deconfined matter; initial conditions are described in text) on $s^{1/2}$. Note that at SPS energies the hadron and a possible mixed phase (not included here) can give further noticeable contributions to the thermal yield

Also displayed in Fig. 1 are rough estimates of the thermal signal from purely deconfined matter assuming boost-invariant expansion. The initial parameters for RHIC and LHC energies are described below. For SPS energies we take the initial temperature $T_i = 200$ MeV at initial time $\tau_i = 1$ fm/c, which are compatible with the observed final pion rapidity densities. Note that the thermal yield estimates depend sensitively on the assumed initial parameters. In agreement with recent findings the thermal dilepton signal is up to two orders of magnitude below the correlated open charm decay dileptons in a wide range of invariant masses at LHC, RHIC [7] and SPS energies. Therefore, there is nowhere a preferred energy region; at high beam energies, however, one expects clearer deconfinement effects due to temperatures far above the confinement temperature.

The results displayed in Fig. 1 cover the full phase space. Any detector acceptance will suppress the various sources differently [8]. Energy losses of heavy quarks propagating through deconfined matter [9] reduce also the open charm and bottom decay yields above $M = 2$ GeV [5,10,11]. Notice that with increasing invariant mass the thermal yield drops exponentially while, for instance, the Drell-Yan yields drops less, i.e. like a power law.

3 Transverse momentum cuts

From all of these considerations the urgent problem arises whether one can find such kinematical gates which enable one to discriminate the thermal signal against the large decay background. Since the kinematics of heavy meson production and decay differs from that of thermal dileptons, one can expect that special kinematical restrictions superimposed on the detector acceptance will be useful for finding the needed window for observing thermal dileptons in the intermediate mass continuum region. In particular, experimental cuts on the rapidity gap between the leptons can reduce considerably the charm decay background [7]. As demonstrated recently [8], the measurement of double differential dilepton spectra as a function of the transverse pair momentum $Q_\perp$ and transverse mass $M_\perp = \sqrt{M^2 + Q_\perp^2}$ within a narrow interval of $M_\perp$ also offers the chance to observe thermal dileptons at LHC. In the present note we show that a large enough low-$p_\perp$ cut on single electrons suppresses the mentioned background processes and opens a window for the thermal signal in the invariant mass distribution. We take into account the acceptance of the ALICE detector at LHC: the single electron pseudo-rapidity is limited to $|\eta_e| \leq 0.9$ and an overall low-$p_\perp$ cut of 1 GeV is applied (we do not impose the earlier planned restriction $p_\perp < 2.5$ GeV). We are going to study systematically the effect of enlarging the low-$p_\perp$ cut on single electrons in the invariant-mass dilepton spectra at $\sqrt{s} = 5500$ GeV.

Since the energy of individual decay electrons or positrons has a maximum of about 0.88 (2.2) GeV in the rest frame of the decaying D (B) meson, one can expect to get a strong suppression of correlated decay lepton pairs by choosing a high enough low-momentum cut $p_\perp^{\min}$ on the individual leptons in the mid-rapidity region. For thermal leptons stemming from deconfined matter there is no such upper energy limit and for high temperature the thermal yield will not suffer such a drastically suppression by the $p_\perp^{\min}$ cut as the decay background. To quantify this effect we perform Monte Carlo calculations generating dileptons from the above mentioned sources. We first employ the transparent lowest-order calculations and then present more complete PYTHIA simulations.

3.1 Dilepton sources

3.1.1 Heavy quark production and decay

We employ here the leading order QCD processes $gg \to Q\bar{Q}$ and $q\bar{q} \to Q\bar{Q}$ for heavy quark production and simulate higher order corrections by an appropriate constant K factor. The number of $Q\bar{Q}$, produced initially with momenta $p_{\perp 1} = -p_{\perp 2} = p_\perp$ at rapidities $y_{1,2}$ in central AA collisions can be calculated by

$$dN_{Q\bar{Q}} = T_{AA}(0)\, \mathcal{K}_Q\, H(y_1, y_2, p_\perp)\, dp_\perp^2\, dy_1\, dy_2, \quad (1)$$

$$H(y_1, y_2, p_\perp) = x_1\, x_2 \left\{ f_g(x_1, \hat{Q}^2)\, f_g(x_2, \hat{Q}^2) \frac{d\hat{\sigma}_g^Q}{d\hat{t}} + \sum_{q\bar{q}} \Big[f_q(x_1, \hat{Q}^2)\, f_{\bar{q}}(x_2, \hat{Q}^2) + f_q(x_2, \hat{Q}^2)\, f_{\bar{q}}(x_1, \hat{Q}^2) \Big] \frac{d\hat{\sigma}_q^Q}{d\hat{t}} \right\}, \quad (2)$$

where $\hat{\sigma}_{q,g}^Q / d\hat{t}$ are elementary cross sections (see for details [4,7]), $f_{g,q,\bar{q}}(x, \hat{Q}^2)$ denote the parton structure functions, $x_{1,2} = m_\perp \left(\exp\{\pm y_1\} + \exp\{\pm y_2\}\right)/\sqrt{s}$ and $m_\perp =$

$\sqrt{p_\perp^2 + m_Q^2}$. As heavy quark masses we take $m_c = 1.5$ GeV and $m_b = 4.5$ GeV. We employ the HERA supported structure function set MRS D-' [3] from the PDFLIB at CERN. Nuclear shadowing effects are not needed to be included for our present order of magnitude estimates. The overlap function for central collisions is $T_{AA}(0) = A^2/(\pi R_A^2)$ with $R_A = 1.2A^{1/3}$ fm and $A = 200$. From a comparison with results of [7] we find the scale $\hat{Q}^2 = 4m_Q^2$ and $\mathcal{K}_Q = 2$ as most appropriate. We employ a delta function fragmentation scheme for the heavy quark conversion into D and B mesons. Dilepton spectra from correlated decays, i.e., $D(B)\bar{D}(\bar{B}) \to e^+Xe^-\bar{X}$, are obtained from a Monte Carlo code which utilizes the inclusive primary electron energy distribution as delivered by JETSET 7.4. The heavy mesons are randomly decayed in their rest system and the resulting electrons then boosted appropriately. The average branching ratio of $D(B) \to e^+X$ is taken as 12 (10)% [12].

3.1.2 Drell-Yan process

Similar to heavy quarks, our calculations of the Drell-Yan pairs are based on the lowest order $q\bar{q} \to e^+e^-$ process with appropriate K factor. For the Drell-Yan production process of leptons at rapidities y_+ and y_- and transverse momenta $p_{\perp+} = -p_{\perp-} = p_\perp$ we have [5]

$$dN_{l\bar{l}}^{DY} = T_{AA}(0)\,\mathcal{K}_{DY}\,L(y_+, y_-, p_\perp)\,dp_\perp^2\,dy_+\,dy_-, \quad (3)$$

$$L(y_+, y_-, p_\perp) = \sum_{q,\bar{q}} e_q^2\,x_1x_2\left[f_q(x_1,\hat{Q}^2)\,f_{\bar{q}}(x_2,\hat{Q}^2) + f_q(x_2,\hat{Q}^2)\,f_{\bar{q}}(x_1,\hat{Q}^2)\right]\frac{d\hat{\sigma}_q^{l\bar{l}}}{d\hat{t}}, \quad (4)$$

with $d\hat{\sigma}_q^{l\bar{l}}/d\hat{t} = \frac{\pi\alpha^2}{3}\mathrm{ch}(y_+ - y_-)/\left(2p_\perp^4[1+\mathrm{ch}(y_+-y_-)]^3\right)$, $x_{1,2} = p_\perp\left(\exp\{\pm y_+\} + \exp\{\pm y_-\}\right)/\sqrt{s}$, $\alpha = 1/137$, $\hat{Q}^2 = x_1x_2s = M^2$, e_q as fractional charges of u, d, s, c quarks, and $\mathcal{K}_{DY} = 1.1$ [3] (for smaller values of M a larger K factor seems appropriate [13], but for our aim such variations are negligible).

3.1.3 Thermal yield

In case of thermal emission of dileptons from deconfined matter the needed distribution of leptons with respect to rapidities $y_\pm$ and transverse momenta $p_{\perp\pm}$ reads [8]

$$dN = \frac{\alpha^2 R_A^2}{4\pi^4}F_q\int d\tau\tau\;K_0\left(\frac{M_\perp}{T}\right) \times\lambda_q^2\,d^2p_{\perp+}d^2p_{\perp-}dy_+dy_- \quad (5)$$

with $F_q = \sum_q e_q^2 = \frac{2}{3}$ for u,d,s quarks, K_n as modified Bessel function of nth order, and with dilepton transverse mass $M_\perp^2 = p_{\perp+}^2 + p_{\perp-}^2 + 2p_{\perp+}p_{\perp-}\mathrm{ch}(y_+ - y_-)$. The integration is to be performed on the proper time τ of the longitudinally expanding deconfined matter with temperature $T(\tau)$ and quark fugacity $\lambda(\tau)$ [4]. Our choice of initial conditions for produced deconfined matter is based on the estimates of [4,14] for the mini-jet plasma which are similar to the self-screened parton cascade model [15]. We take as main set of parameters the initial temperature $T_i = 1000$ MeV, gluon fugacity $\lambda_i^g = 0.5$, and light quark fugacity $\lambda_i^q = \frac{1}{5}\lambda_i^g$ of the parton plasma formed at LHC at initial time $\tau_i = 0.2$ fm/c. For the sake of definiteness we assume full saturation at confinement temperature $T_c = 170$ MeV and a quadratic time dependence of $\lambda^{q,g}(\tau)$ according to the studies [4,16].

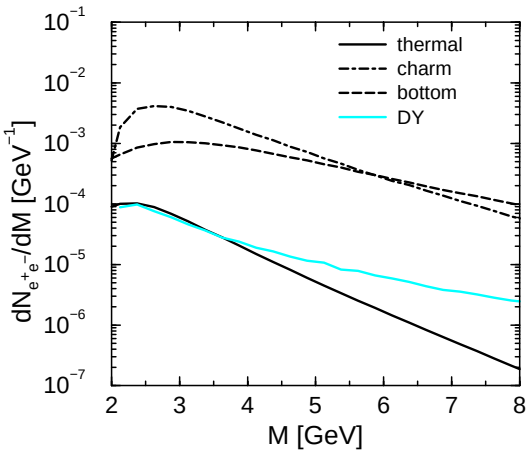

Fig. 2. The invariant mass spectra of dileptons from the Drell-Yan process, and charm and bottom decays, and thermal emission. The single-electron low transverse momentum cut is $p_\perp^{\min} = 1$ GeV

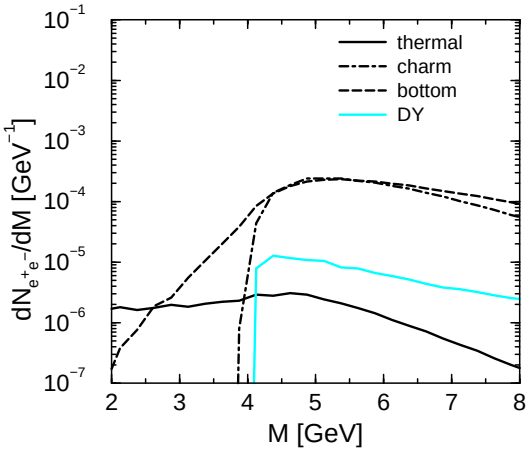

Fig. 3. The same as in Fig. 2, but $p_\perp^{\min} = 2$ GeV

3.2 Results of lowest-order calculations

The results of our lowest-order calculations of the invariant mass spectrum for various values of $p_\perp^{\min}$ are displayed in Figs. 2–4. Comparing Figs. 2 and 3, one observes that already the cut $p_\perp^{\min} = 2$ GeV causes a strong suppression of the correlated charm decay and Drell-Yan background in the region $M \le 2p_\perp^{\min}$. The above value of the

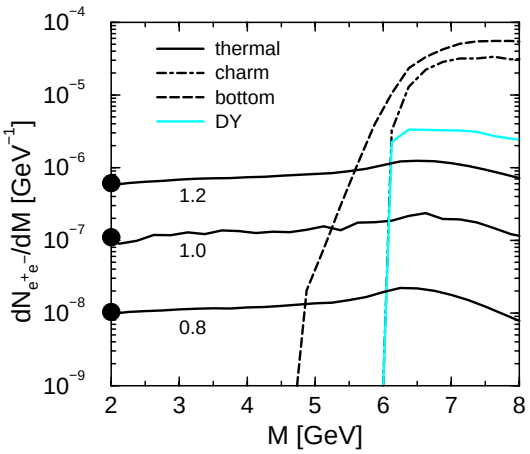

Fig. 4. The same as in Fig. 2, but $p_\perp^{\min} = 3$ GeV and various initial temperatures (in units of GeV) as indicated by the labels. The fat dots indicate the estimates of the low-M thermal plateau according to (6)

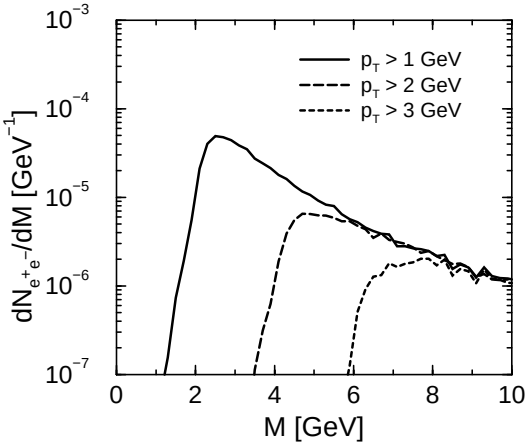

Fig. 5. The invariant mass spectra of dileptons from the Drell-Yan process for $p_\perp^{\min} = 1$, 2 and 3 GeV (from left to right). The curves depict results of PYTHIA with default switches

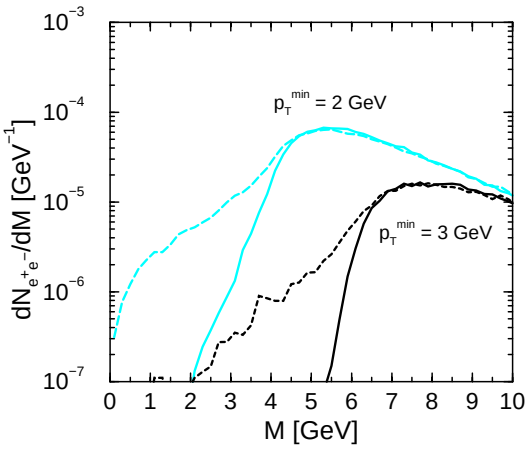

Fig. 6. The invariant mass spectra of dileptons from correlated open bottom meson decays for $p_\perp^{\min} = 2$ and 3 GeV. The curves depict results of PYTHIA (dashed curves: default switches, solid curves: without initial state radiation)

invariant mass threshold can be estimated by using the relation $M^2 = 2p_{\perp+}p_{\perp-}[\mathrm{ch}(y_+ - y_-) - \cos(\phi_+ - \phi_-)]$, where $\phi_\pm$ denote the azimuthal angles of the leptons in the transverse plane. In order to exceed the cut $p_\perp^{\min}$ most easily, the decay leptons should go parallel to the parent heavy mesons, which in turn are back-to-back (in the transverse plane) in lowest order processes. As a consequence, $\cos(\phi_1 - \phi_2) \approx -1$ and the minimum invariant mass becomes $M^{\min} \approx 2p_\perp^{\min}$ for such decay pairs. For correlated bottom decay the electron energy is larger in the meson rest system and both leptons can easily overcome the threshold $p_\perp^{\min}$ without such strong back-to-back correlation. Selecting, however, electrons with $p_\perp > p_\perp^{\min} = 3$ GeV one can also get the corresponding threshold like behavior for the lepton pairs from correlated bottom decay, see Fig. 4. Therefore the thermal signal becomes clearly visible for such a value of $p_\perp^{\min}$ due to the strong suppression of the considered background channels.

The threshold behavior does not change if we include in our calculations energy loss effects of heavy quarks in deconfined matter [9]. Such effects cause mainly a suppression of the decay contributions (cf. [5,10,11]). We also mention that shadowing effects, not included in our Drell-Yan and heavy quark production estimates, will diminish these yields somewhat. (In the mini-jet estimates of our initial conditions [4] shadowing effects are already included).

3.3 Results from PYTHIA

The lowest order Drell-Yan yield has anyway $M^{\min} = 2p_\perp^{\min}$. From the above given relations for M and $M_\perp$ one can derive the inequality $M \geq 2p_\perp^{\min}\sqrt{1 - \left(\frac{Q_\perp}{2p_\perp^{\min}}\right)^2}$. This relation tells us that in the region $M < 5$ (4) GeV only pairs with total transverse momentum $Q_\perp > 3.25$ (4.5) can contribute if $p_\perp^{min} = 3$ GeV. Since the next-to-leading order Drell-Yan distribution $dN/dM^2dQ_\perp^2dY$ drops from $Q_\perp \approx 0$ to 3 - 4 GeV by nearly three orders of magnitude [13] one can estimate a small higher order Drell-Yan contribution in the small-M region. To quantify the smearing of the threshold effect by an intrinsic $p_\perp$ distribution of initial partons we perform simulations with the event generator PYTHIA (version 6.104 [17]) with default switches. Results are diplayed in Fig. 5 and show that the sharp threshold effect from the above lowest-order Drell-Yan process is indeed somewhat smeared out, however, the small-M region is still clean. It turns out that the initial state radiation of partons before suffering a hard collision is the main reason for rising the pair $Q_\perp$ and for smearing out the sharp threshold effect, while the intrinsic $p_\perp$ distribution of partons causes minor effects.

Let us now consider heavy quark pairs. Here, the intrinsic $p_\perp$ distribution, and both initial and final state radiations of the partons can cause a finite $Q_\perp$ and thus destroy the strong back-to-back correlation, i.e. $p_{\perp 1} \neq p_{\perp 2}$. In Fig. 6 we show results of simulations with PYTHIA for the bottom channel. The resulting primary dileptons from

all correlated open bottom mesons are displayed. One observes that the initial state radiation causes a pronounced smearing of the threshold effect discussed above. Without the initial state radiation, as implemented in PYTHIA, the threshold effect is recovered. The intrinsic $p_\perp$ distribution and final state radiation are negligible. The conclusion of such studies is that an enlarged value of $p_\perp^{\min}$ is necessary to keep clean the low-M region from open bottom decay products. For charm the smearing effect due to initial state radiation in PYTHIA is efficiently suppressed by the large enough low-$p_\perp$ cut of $p_\perp^{\min} = 3$ GeV. The different behavior of charm and bottom stem from the fact that the bottom-$p_\perp$ distribution is much wider. As a consequence, the bottom is evolved in the average to much larger values of $\hat{Q}^2$ thus experiencing stronger kicks by initial state radiation. In agreement with our previous findings [5], bottom therefore causes the most severe background processes at LHC energies.

With PYTHIA also the dileptons from single decay chain of open bottom are accessible. This channel provides a contribution peaking at 1.5 GeV; the cut $p_\perp^{\min} = 3$ GeV pushes all invariant masses below 3 GeV. Therefore, unless enlarging $p_\perp^{\min}$ considerably, it will be difficult to suppress kinematically the background below the thermal signal at invariant masses $M < 3$ GeV. Probably explicit identification and subtraction of the bottom contribution is needed in this region. Otherwise one should stress that the thermal signal of deconfined matter is expected to exceed the thermal hadron signal at $M > 2$ GeV [16]. Hence the region of small values of M is not interesting in this respect.

We conclude this subsection by mentioning that further differences between our above lowest-order calculations and the PYTHIA simulations stem from slightly different charm/bottom masses, different fragmentation schemes and decay chains. We have checked that for the same masses, the same fragmentation scheme (i.e. independent fragmentation) and PYTHIA without intrinsic $p_\perp$ distribution and without initial/final state radiation, PYTHIA then reproduces our calculations. According to our experience, the stringent kinematical cuts amplify small differences in various code versions. We do not intent here to present a detailed prediction of the dilepton yield, but rather to demonstrate that an observation of a thermal signal from deconfined matter is not excluded. Therefore, we do not attempt any fine tuning of the codes to reproduce the bulk of data in pp and pA reactions.

3.4 Physical information encoded in the continuum spectrum

The thermal dilepton signal with single-electron low-momentum cut-offs $p_\perp^{\min} = 2 - 3$ GeV exhibits an approximate plateau in the invariant mass region 2 GeV $\leq M \leq 2p_\perp^{\min}$ (see Fig. 4). The physical information encoded in the height of the plateau can be estimated by

$$\frac{dN}{dM^2 dY} = 3\frac{\alpha^2 R_A^2}{4\pi^2} F_q \left(\tau_i \lambda_i^q T_i^3\right)^2 \times 2\int_{2p_\perp^{\min}/T_i}^{\infty} dx \left(\frac{8}{x^2}+1\right) \times K_3(x) \frac{x - 2p_\perp^{\min}/T_i}{\sqrt{x^2 - (M/T_i)^2}} \quad (6)$$

(cf. Appendix for details of the derivation). By explicit calculation of this equation and as seen in Fig. 4, the height of the plateau depends sensitively on the initial temperature T_i and quark fugacity λ_i^q. This dependence can be used to get physical information on the early and hot stage of the parton matter. In particular, a variation of the initial temperature within the interval 0.8 – 1.2 GeV, expected as possible range of parton matter formed at LHC energies, leads to a considerable change of the plateau height up to an order of magnitude. Therefore, once an identification and a measurement of the thermal dilepton spectrum in the intermediate mass continuum spectrum is possible, it delivers some implicit information on the initial and very hot stages of the parton matter.

4 Summary

In summary we analyze the beam energy dependence of various expected sources of dileptons in ultrarelativistic heavy-ion collisions. Already at $\sqrt{s} > 20$ GeV a copious production of charm gives rise to a dominant contribution to the dilepton spectrum at intermediate invariant mass. Taking into account the ALICE detector acceptance we study also systematically the effect of single-electron transverse momentum cuts. We find a threshold like behavior of the invariant mass spectra of dileptons from primary correlated charm and bottom decays and Drell-Yan yield as well: these sources are suppressed at $M < M^{\min} \approx 2p_\perp^{\min}$ for $p_\perp^{\min} > 3$ GeV. In contrast to this, the thermal dilepton signal exhibits a plateau in this region which offers the opportunity to identify them and to gain information on the initial stages of deconfined matter at LHC energies. The same mechanism also works at RHIC energies, however the expected count rates are too small to make such a strategy feasible. The complex decay chains of heavy mesons, in particular open bottom, and the resulting combinatorial background make an explicit identification of the "hadronic cocktail" very desirable to allow a safe identification of the thermal signal.

Acknowledgements. We thank P. Braun-Munzinger who initiated this investigation. Stimulating discussions with Z. Lin, R. Vogt, G. Zinovjev are gratefully acknowledged. O.P.P. thanks for the warm hospitality of the nuclear theory group in the Research Center Rossendorf. The work is supported by BMBF grant 06DR829/1.

Appendix

We rewrite the general expression (5) for the thermal dilepton spectrum as

$$\frac{dN}{dM^2} = \frac{\alpha^2 R_A^2}{4\pi^4} F_q \int d\tau \tau d^2p_+ d^2p_- dy_+ dy_- \, K_0\left(\frac{M_\perp}{T}\right) \lambda_q^2 \times\delta\left[M^2 - 2p_{\perp+}p_{\perp-}\{\cosh(y_+ - y_-) - \cos(\phi_+ - \phi_-)\}\right] \quad (7)$$

and arrive after three integrations at

$$\frac{dN}{dM^2} = \frac{\alpha^2 R_A^2}{4\pi^2} F_q \int dY dM_\perp^2 \; d\tau\, \tau\, K_0\left(\frac{M_\perp}{T(\tau)}\right) \times\lambda_q^2(\tau)\, \frac{1}{\pi} \mathrm{I}(M, M_\perp, p_\perp^{\min}) \quad (8)$$

with

$$\mathrm{I}(M, M_\perp, p_\perp^{\min}) = 2\int_{x_1}^{x_2} dx \frac{1}{M_\perp} \frac{x^2\, \mathrm{F}(\phi,k) + M_\perp^2[\mathrm{E}(\phi,k) - \mathrm{F}(\phi,k)]}{\sqrt{(x^2 - Q_\perp^2)(M_\perp^2 - x^2)}}\,, \quad (9)$$

where E and F stands for the incomplete elliptic integrals

$$\mathrm{F}(\phi,k) \equiv \int_0^{\sin\phi} \frac{dt}{\sqrt{(1-t^2)(1-k^2t^2)}}, \qquad \mathrm{E}(\phi,k) \equiv \int_0^{\sin\phi} \frac{(1-k^2t^2)\; dt}{\sqrt{(1-t^2)(1-k^2t^2)}} \quad (10)$$

with $\phi = \arcsin\left(\frac{\Delta(x)}{Q_\perp}\right)$ and $k = \frac{Q_\perp}{M_\perp}$, and $\Delta(x) = \min(x - 2p_\perp^{\min}, Q_\perp)$, $x_1 = \max(2p_\perp^{\min}, Q_\perp)$, $x_2 = M_\perp$. In the special case $p_\perp^{\min} = 0$ the expression $\mathrm{I}(M, M_\perp, p_\perp^{\min})$ becomes π. In the small-M region one can approximate $\Delta(x) \approx M_\perp - 2p_\perp^{\min}$ being independent of x. Then the x integration yields

$$\mathrm{I}(M, M_\perp, p_\perp^{\min}) \approx 2\Big(\mathrm{E}(\pi/2, \sqrt{1-k^2})\mathrm{F}(\phi,k) + \mathrm{F}(\pi/2, \sqrt{1-k^2})\mathrm{E}(\phi,k) - \mathrm{F}(\pi/2, \sqrt{1-k^2})\mathrm{F}(\phi,k)\Big). \quad (11)$$

Since for small M also $Q_\perp/M_\perp \approx 1$ holds, one can use $\mathrm{E}(\phi,0) = \mathrm{F}(\phi,0) = \phi$ and $\mathrm{E}(\phi,1) = \sin\phi$ and finds

$$\mathrm{I}(M, M_\perp, p_\perp^{\min}) \approx \pi \frac{M_\perp - 2p_\perp^{\min}}{Q_\perp}. \quad (12)$$

For $p_\perp$ cuts larger than 2 GeV one gets from (8, 12) the approximate expression (6) when approximating the τ integration appropriately [8].

References

1. E.V. Shuryak, Phys. Rep. **61**, 71 (1980)
2. P.V. Ruuskanen, in *Quark-Gluon Plasma*, edited by R. Hwa, (World Scientific, Singapore 1990), p. 519
3. A.D. Martins, W.J. Stirling, R.G. Roberts, Phys. Lett. B **306**, 145 (1993)
4. B. Kämpfer, O.P. Pavlenko, Phys. Lett. B **391**, 185 (1997)
5. B. Kämpfer, O.P. Pavlenko, K. Gallmeister, Phys. Lett. B **419**, 412 (1998)
6. P. Braun-Munzinger, D. Miskowiec, A. Drees, C. Lourenço, Eur. Phys. J. C **1**, 123 (1998)
7. S. Gavin, P.L. McGaughey, P.V. Ruuskanen, R. Vogt, preprint LBL-37981, Phys. Rev. C **54**, 2606 (1996)
8. K. Gallmeister, B. Kämpfer, O.P. Pavlenko, Phys. Rev. C **57**, 3276 (1998)
9. R. Baier et al., Phys. Lett. B **345**, 277 (1995), Nucl. Phys. B **483**, 291 (1997), Nucl. Phys. B **484**, 265 (1997), Phys. Rev. C **58**, 1706 (1998)
10. E.V. Shuryak, Phys. Rev. C **55**, 961 (1997)
11. Z. Lin, R. Vogt, X.-N. Wang, Phys. Rev. C **57**, 899 (1998)
12. R.M. Barnett et al. (Particle Data Group), Phys. Rev. D **54**, 1 (1992)
13. S. Gavin, S. Gupta, R. Kauffman, P.V. Ruuskanen, D.K. Srivastava, R.L. Thews, Int. J. Mod. Phys. A **10**, 2961 (1995)
14. K.J. Eskola, K. Kajantie, P.V. Ruuskanen, Phys. Lett. B **332**, 191 (1994); K.J. Eskola, Nucl. Phys. A **590**, 383c (1995)
15. K.J. Eskola, B. Müller, X.-N. Wang, Phys. Lett. B **374**, 20 (1996)
16. B. Kämpfer, O.P. Pavlenko, A. Peshier, G. Soff, Phys. Rev. C **52**, 2704 (1995)
17. T. Sjöstrand, Comp. Phys. Commun. **82**, 74 (1994); cf. also http://thep.lu.se/tf2/staff/torbjorn/Pythia.html